

DESIGN PROCESS OF AN UAV AIRCRAFT FOR AIAA DBF 2013 COMPETITION

Murat Senipek¹, Metehan Yayla, Afif Umur
Limon, Ramin Rouzbar, Yosheph Yosheph,
Ugur Kalkan, Niyazi Senol, Ezgi Akel, Osman
Gungor, Batuhan Hos, Ayse Usta, Ismail O.
Uzunlar, and S. Burak Sarsilmaz

D. Funda Kurtulus²
Middle East Technical University
Ankara, Turkey

Middle East Technical University
Ankara, Turkey

ABSTRACT

The main objective of this paper is to present the design and manufacturing procedure of for an aircraft for AIAA DBF 2013 Competition. The content of the paper is divided into the introduction of the mission, design process, manufacturing process and performance results. The design stage is divided into 3 categories as Conceptual Design, Preliminary Design, and Detailed Design [Raymer, 1999]. Based on this design analysis, the unmanned aircraft is manufactured. Several flight tests are made after the manufacturing stage. Based on the flight test results, the design is improved such a way that the final design satisfies all mission requirements. In each stage of the design, several tools are used in order to aid the design process such as: Figure of Merit, CFD analysis and different Optimization Tools. After finalizing the aircraft design, performance results are analyzed. Upon completing all these steps, it is found that the final aircraft is excellent enough to satisfy all required missions governed by AIAA DBF 2013 committee.

INTRODUCTION

As stated in AIAA DBF 2013 Competition rules, the aim was to design a Joint Strike Fighter. The design should satisfy three different missions, as stated below:

1. Short Take-Off

Successful short take-off is required within the prescribed area and the goal is to complete as many number of successful laps as possible.

2. Stealth Mission

Successful short take-off is required within the prescribed area and the purpose is to carry as much as internal payloads (Mini Max).

3. Strike Mission

Successful short take-off is required within the prescribed area and the aim is to carry the missiles for three successfully flown laps. Payload configuration will be a random draw of internal and external payloads. The configuration will be determined just before the flight by rolling a dice. Therefore there were six number of possible configuration of external payloads.

In addition to the above mission requirements, several design constraints are also imposed in the design such as: current limitation and mission score. Each mission is scored differently. Before beginning the design, score analysis is performed in order to obtain a good score at the end of the design process.

¹Undergraduate student in Department of Aerospace Engineering METU Email: muratsenipek@gmail.com

²Assoc. Prof. Dr. in Department of Aerospace Engineering METU Email: dfunda@ae.metu.edu.tr

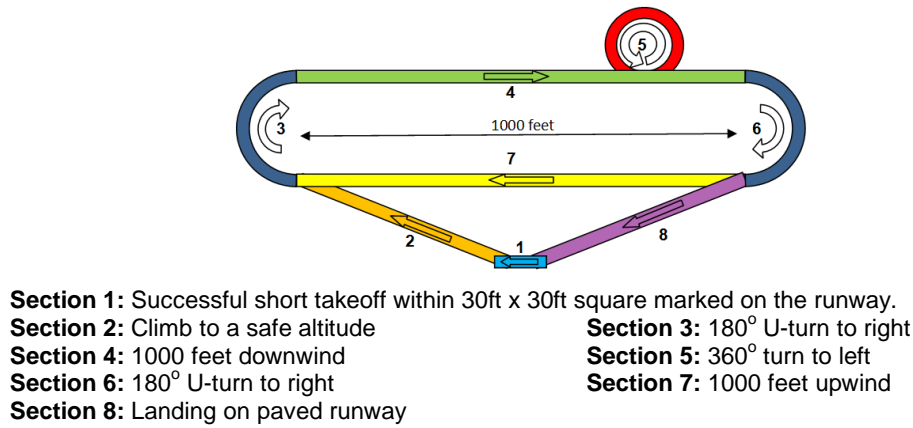


Figure 1: Mission flight course

METHOD

Total Score Calculation

The total flight score for each team is calculated as given in Eq. 1:

$$\text{SCORE} = \frac{\text{Written Report Score} \times \text{Total Flight Score}}{\text{RAC}} \quad \text{Eq.1}$$

The total flight score (TFS) is calculated as:

$$\text{Total Flight Score} = M1 + M2 + M3 \quad \text{Eq.2}$$

Rated Aircraft Cost (RAC) is calculated as shown in Eq.3:

$$\text{RAC} = \sqrt{\text{EW} \times \text{SF}} / 10 \quad \text{Eq.3}$$

where

$$\text{Empty Weight (EW)} = \max(\text{EW1}, \text{EW2}, \text{EW3})$$

$$\text{Size Factor (SF)} = X_{\max} + 2Y_{\max}$$

Sensitivity Analysis

From the score evaluation obtained from each mission, it is found that the major contribution comes from the 3rd mission. In addition of this, determination the most crucial parameter for total flight score in the design should be considered. Sensitivity analysis is done by changing the parameters affecting the score and analyzing the optimum score. Detail of the sensitivity analysis is shown in Figure 1.

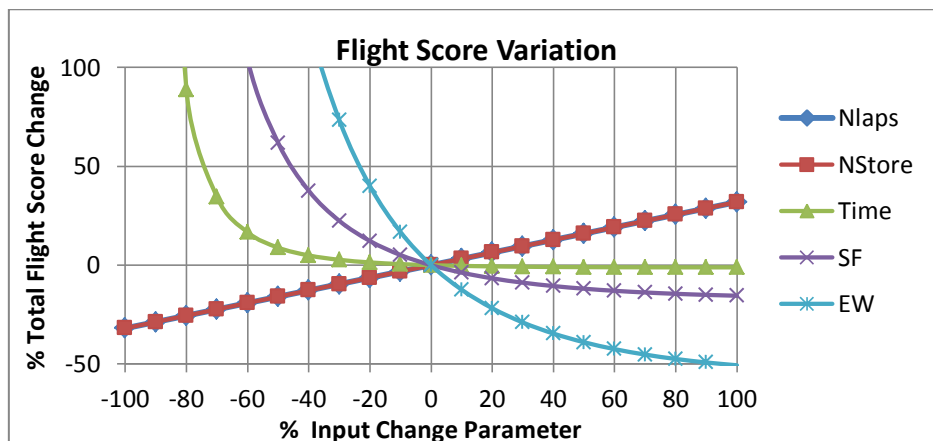

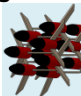
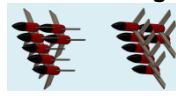



Figure 2 Sensitivity Analysis Performed for AIAA DBF Competition

Figure of Merits

In order to get a better idea about which design parameter should be chosen, a comparison should be made. The comparison is made by aid of Figure of Merits. In this FOM, all candidates for design are considered with their contribution to the final design. From each configuration, overall contribution is calculated. At the end of the design, overall contribution is calculated. A criterion which has the highest overall contribution is considered to be the final design. Sample of Figure of Merits used in the design is shown in Table 1.

Table 1: Sample Figure of Merit Used in the Fuselage Design

FOM Chart	Weight	Single Fuselage 	Single Fuselage 	Twin-Fuselage 	Twin-Fuselage 
Surface Drag	0.3	2	3	4	5
Height	0.15	4	3	3	3
Manufacturability	0.1	4	2	5	3
Wing Intersection	0.25	3	3	4	4
Stability	0.2	4	5	2	3
OVERALL	1	3.15	3.3	3.55	3.85

General conceptual design methodology can be described as in Figure 3:

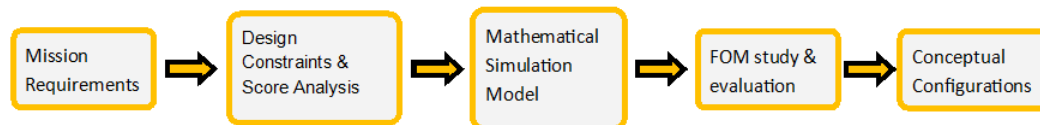


Figure 3: Conceptual Design Methodology

DESIGN PROCESS

As discussed earlier, the design process utilized here divided into three major sections, which are: conceptual design, preliminary design, and detailed design.

Conceptual Design

Conceptual design process is started by analyzing the mission requirements, design constraints, and score analysis. This process is followed by creating a mathematical model for the mission envelopes.

Next, aircraft configuration is determined. By considering the mission goals and score parameters, a detailed Figure of Merit (FOM) study is done by considering the solutions for the design constraints and score analysis. Finally, the conceptual configuration is selected.

In the conceptual design process, aircraft configuration like: aircraft, wing, tail, fuselage, landing gear, and propulsion are determined as Figure 4. Finally, the selected configurations for the conceptual design are: monoplane aircraft, high wing, twin-prop, inverted V-tail, and quadri-cycle landing gear configuration (Şenipek et al., 2013).

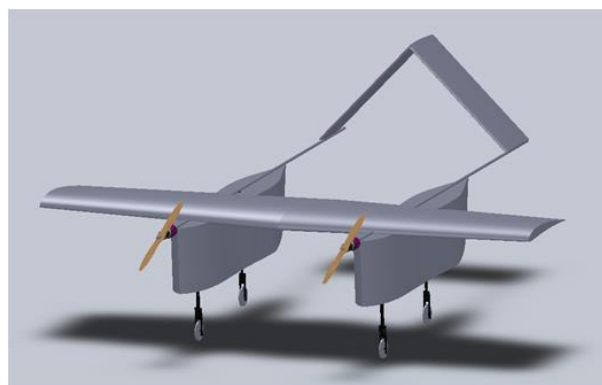


Figure 4: Conceptual Sketch of the Aircraft

Preliminary Design

During this design stage, a more detailed analysis based on the final conceptual design is performed. The geometry of the wing, tail, fuselage, and propulsion selection is decided here. Mathematical model is created in order to estimate the take-off performance (flaps down), turn performance and mission performances for each possible flight envelope. Results obtained from the model improve the initial values for aircraft design parameters. Initial wing loading, thrust to weight ratio and motor type are highly determined from the mathematical model. Mission flight performance is plotted in Figure 5 by using the mathematical model.

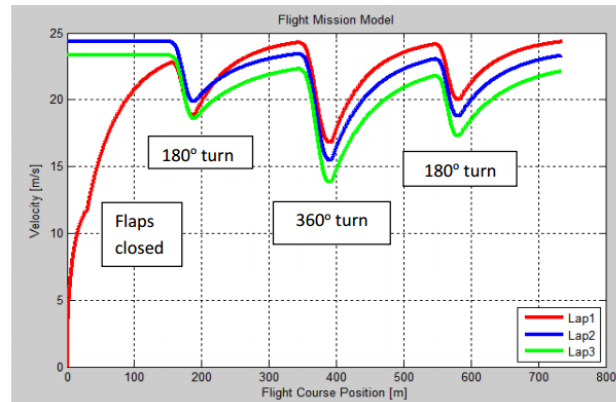


Figure 5: Velocity Profile vs Flight course with Max. Take-off Weight

The wing geometry is determined from wing loading that calculated based on three different constraints like stall speed, max take-off distance, and take-off velocity. From all these constraints, minimum value of wing loading is chosen. Based on this wing loading value, wing geometry is then determined. The determination of geometry of the wing is done by using Raymer's concept for aircraft design.

Airfoil Selection

The airfoil selection is also done in this stage of the design. Over 300 of airfoils are searched. Then the best three airfoils in Table 2 are selected according to the following constraints:

- High maximum lift coefficient with flaps down
- Low zero-lift drag coefficient
- Easy to manufacture

Table 2: Geometry comparison of final selected airfoils

Standard	Thickness (%)	LE Radius (%)	Camber (%)	Maximum t/c
S4180	9.78	1.160	4.36	26.11
FX M2	9.41	0.970	4.78	19.50
SG 6042	10.0	1.121	3.75	33.51

In order to get a good aerodynamic result the analysis performed in FLUENT. Flap down situation is also analyzed for short take-off performance (Figure 6). Flap hinges are positioned at 75% of the chord.

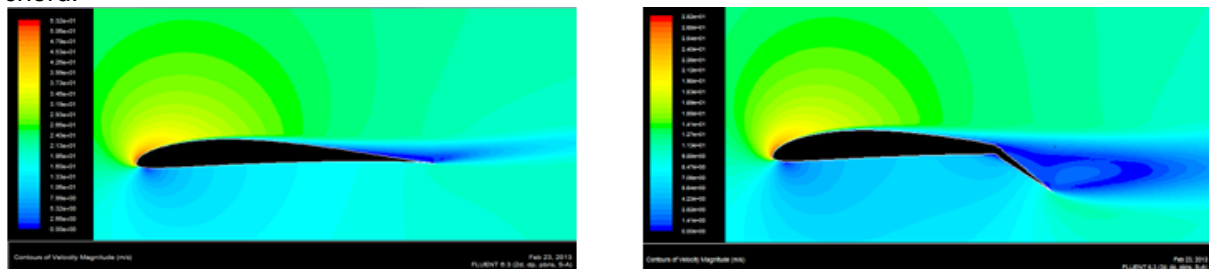


Figure 6 CFD analyses of flaps on (at 75% of the chord; 25deg) and off cases of S4180

From analyses, C_l vs C_d and C_l vs α are drawn. These graphs are shown in Figure 7. The results are also represented for flap on configuration.

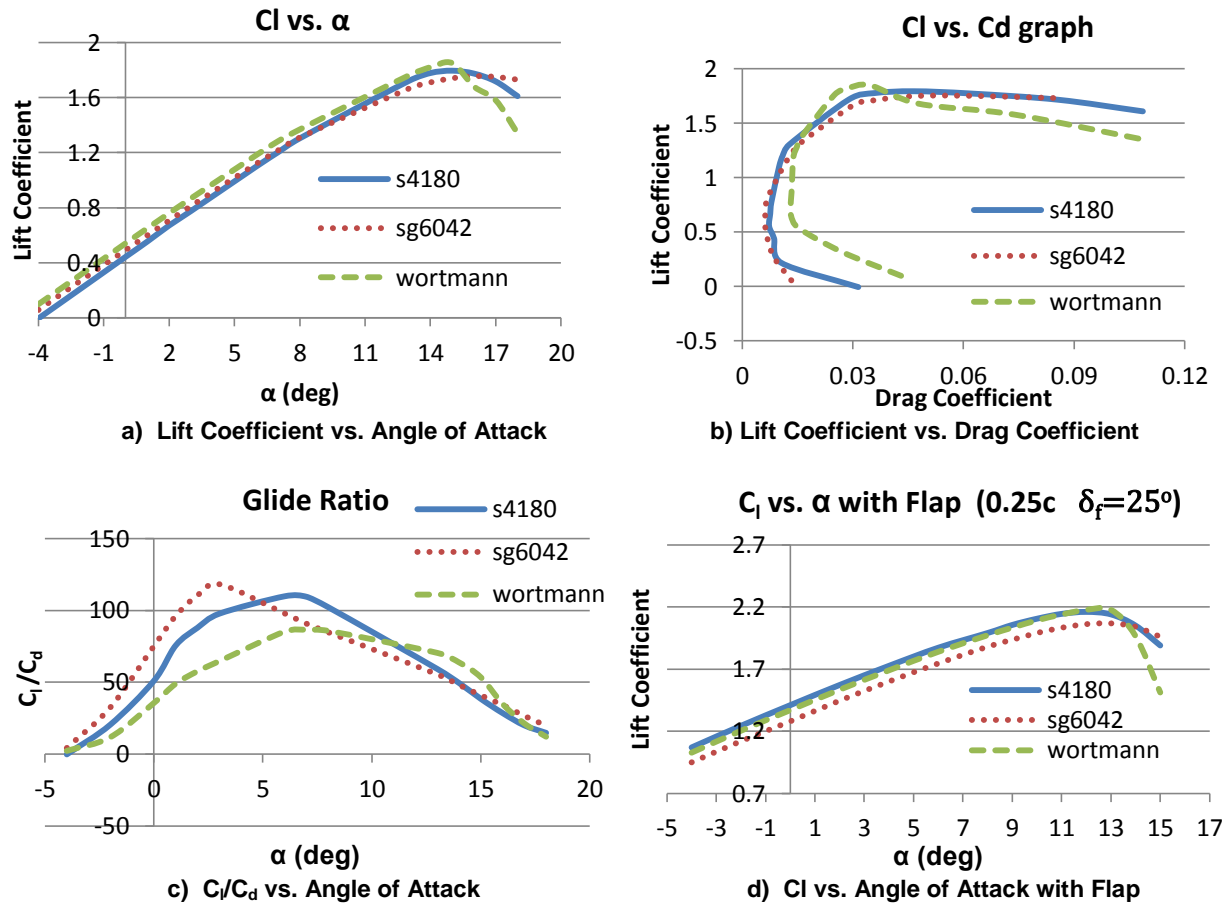


Figure 7: Aerodynamic Coefficients for Different Airfoils

By considering the characteristic during the stall, take-off, lift and drag ratio, and easiness of manufacturing, S4180 airfoil is selected for wing airfoil. However, some modification of the S4180 airfoil is made in order to achieve better aerodynamic results. Modified airfoil properties are summarized in Table 3 in comparison with the real S4180 airfoil. The comparison of the aerodynamic properties between S4180 and modified airfoil are shown in Figure 8.

Similar airfoil selection procedure is also done for sizing the tail of the aircraft. Symmetric and thin NACA 0009 airfoil has been chosen for the tail.

Table 3: S4180 and S4180 modified airfoil geometries

	Thickness (%)	LE Radius (%)	Camber (%)	Maximum t/c Location (%)
S4180	9.78	1.160	4.36	26.11
S4180-modified	10.00	1.373	5.42	22.11

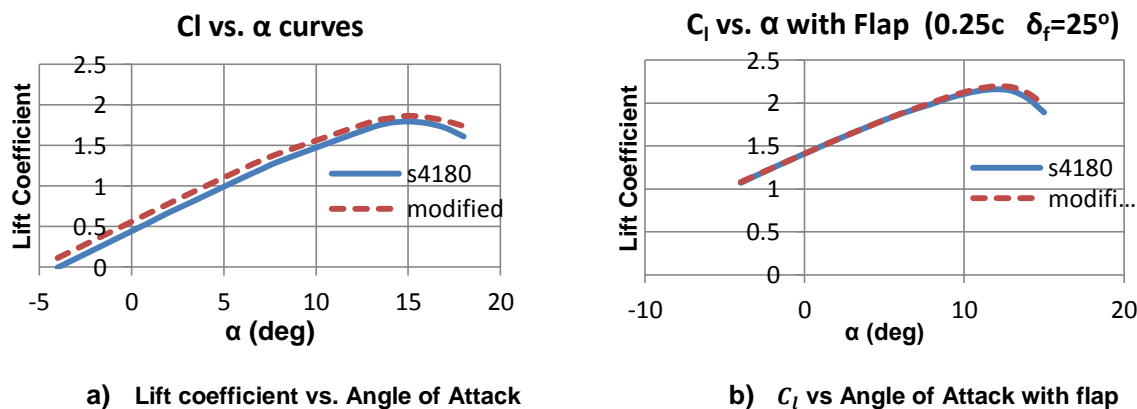
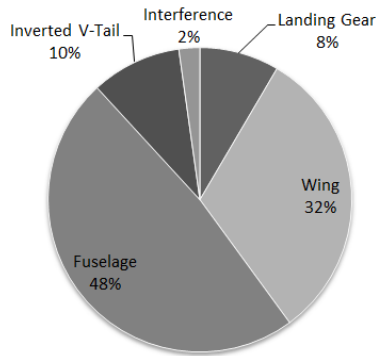


Figure 8: Aerodynamic Coefficients for S4180 and modified airfoil

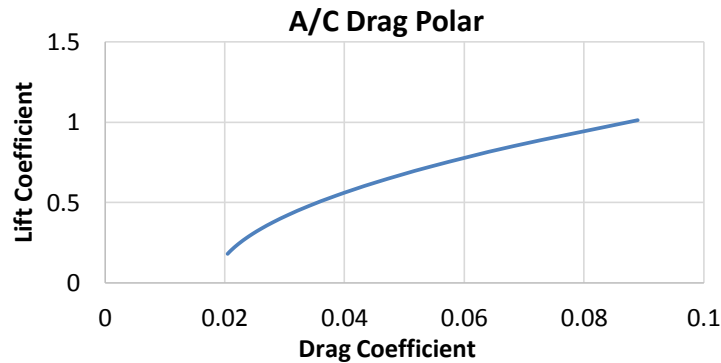
Drag Estimation:

Wing, fuselage, inverted V-tail, and landing gear parasite drag coefficients are estimated separately. Moreover, an interference drag is added in order to compensate the interference aerodynamic effects. Figure 9 shows the percentage of the parasite drag contributions of aircraft components.

Drag contributions of components (Twin Body)**Figure 9:** Parasite Drag contribution of each component of aircraft**Table 4:** Parasite Drag Coefficients for each Dice Configuration

	Mission 1	Mission 2	Mission 3					
			Dice 1	Dice 2	Dice 3	Dice 4	Dice 5	Dice 6
Parasite Drag	0.0182	0.0182	0.0187	0.0188	0.0186	0.0185	0.0187	0.0187

The induced drag of the aircraft is calculated for the cruise flight which has $C_{L_{cruise}} = 0.19$. The total drag polar of the aircraft is shown in Figure 10.

**Figure 10:** Drag polar of the aircraft**Propulsion System Selection:**

Propulsion system consists of twin electric motors, two cells of NiMh battery packs, two ESC (Electronic Speed Controller) and two propellers having opposite pitch. Due to the competition rules the electric current passing through any wire should not exceed 20A.

Since high static thrust is required for short take-off and high speed is required for best score the propulsion system selection is very important topic. Both thrust and maximum velocity is examined while selecting the motor and propeller match. (Mark Drela's QPROP) and some blade element theories are used in order to determine the dynamic thrust routine for each propeller.

Moreover the weight of the total propulsion system is another important topic. Therefore the motors and the number of batteries are also optimized.

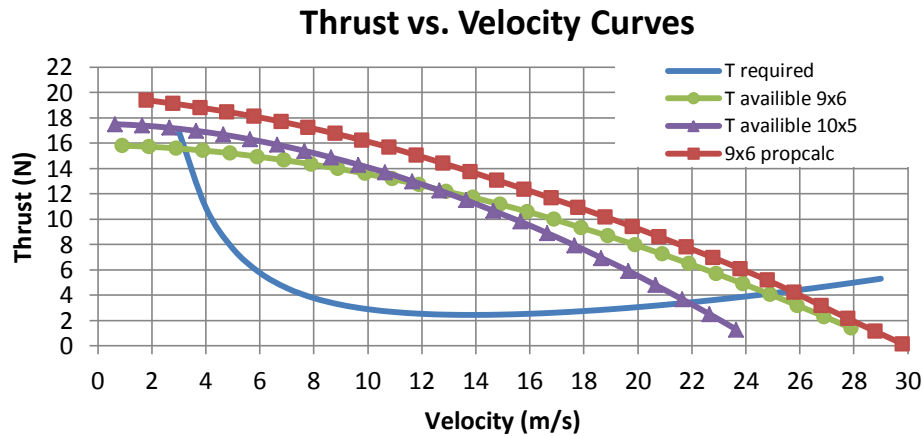


Figure 11: Thrust vs. Velocity curves for aircraft performance

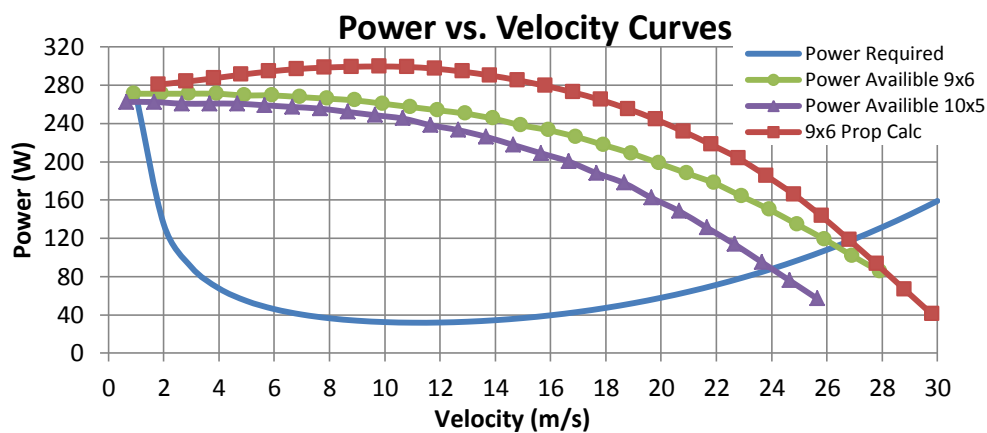


Figure 12: Power vs. Velocity curves for aircraft performance

After these theoretical results the propulsion system is selected as (x2) Hacker A20-12XL Electric Motors, (x2) Hacker MASTERSPIN22 ESC's, (x2) 11 cells of Elite batteries for first two mission and 12 cells of Elite batteries for last mission.

While optimizing the propeller performance and in order to determine the best options a test setup is manufactured. In these setup the current, electrical power, and voltage draw is recorded by a simple electronic circuit, thrust is recorded by 5kg load cell and RPM is calculated by a laser tool.

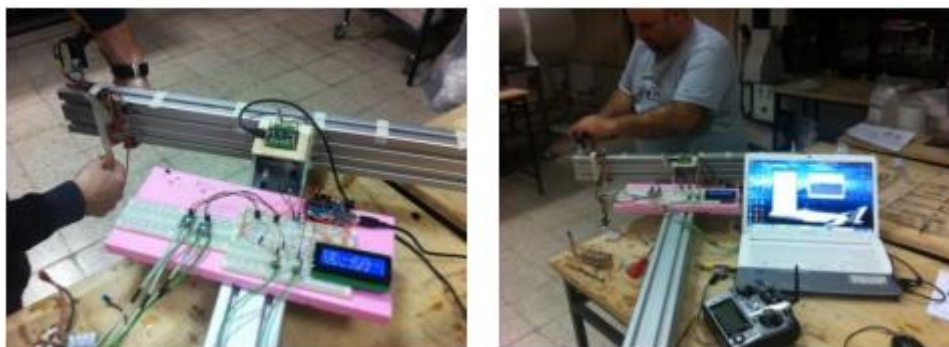


Figure 13: Propulsion system test setup

The parameters are recorded for a 240 seconds of time which is the maximum allowable flight time and results are obtained from these experiments for one motor system are shown in Figure 14.

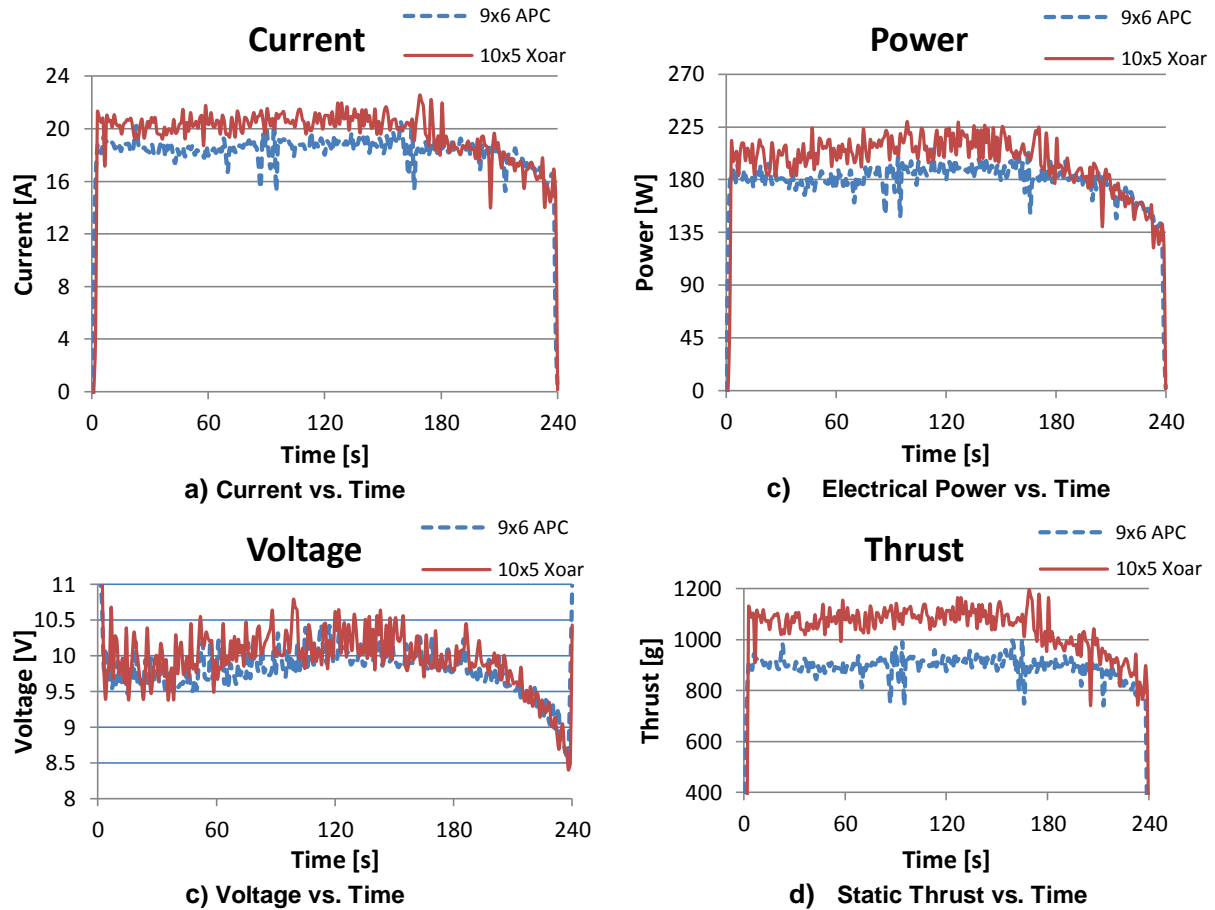


Figure 14: Motor response curves

After these tests and detailed analyses final propeller and battery configurations which are on Table 5 are determined.

Sizing of the control surfaces done by using the relations in Nicolai (2010). General summary of the aircraft components are tabulated in Table 5.

Table 5: Summary of Aircraft Dimensional Parameters

Wing		Inverted V-Tail Properties		Aileron	
Airfoil	Modified	Airfoil	NACA 0009	Span [m]	0.37
Span [m]	1.5	Angle between V	92.314°	% of Chord	25%
M.A.C. [m]	0.341	Span [m]	0.55	Max δ_a	30°
Area [m ²]	0.502	Total Area [m ²]	0.114	Flap	
Aspect Ratio	4.48	Vertical Distance [m]	0.552	Span [m]	0.4
Taper Ratio	0.618	Chord [m]	0.148	% of Chord	22-28%
Oswald's eff.	0.934	Incidence [deg]	-1°	Max δ_f	30°
Static Margin	13%	Motor		Rudder-Vator	
Incidence Angle	1°	Type	A20 6XL	Span [m]	0.523
Twist Angle	2°	Kv	1050	% of Chord	40%
c/4 Sweep	0°	RPM _{max}	12000	Max δ_e	35°
Fuselage		Rm [Ω]	0.075	Electrical System	
Length [m]	0.74	Operating Current [A]	~20	ESC	MASTERSPIN22
Width [m]	0.16	Propellers (M1)	9x6 APC	Servo δ	HS55 – S3117
Height [m]	0.12	Propellers (M2 & M3)	10x5 Xoar	Receiver	FUTABA

Detailed Design:

In this stage of design, a more advanced design stage is considered. The main important concept considered in here are material selection, internal structure of the aircraft, and CFD analysis. Balsa wood is chosen as the main material for the aircraft. This balsa wood is later equipped with carbon boom which acts as a spar. Sizing of the carbon boom is made such that it can handle the impacted load on the aircraft.

One of the mission objectives in AIAA DBF 2013 is to have an aircraft which can carry all payload configurations. In order to have this capability, the wing should be designed such that it can support all the payloads. The location of the external payload is determined by using “*fmincon*” command in MATLAB. The objective function to be minimized is the moment of inertia generated due to external payload while keeping the moment generated to be equal to zero. Based on this optimization tools, the location of the external payload is determined.

In this stage of design, a more detailed of CFD analysis is made in order to see how the flow around the aircraft looks like. Detailed of CFD analysis is shown in Figure 15.

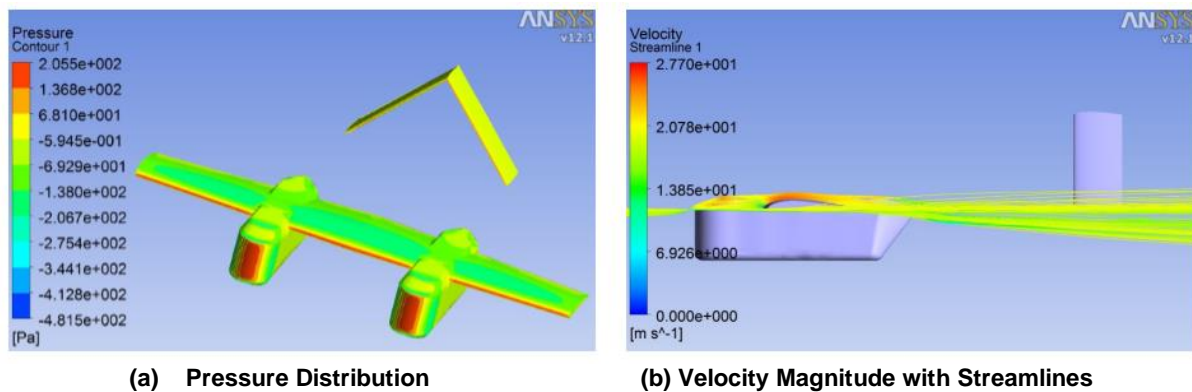


Figure 15: CFD Analysis for Cruise Condition

Stability:

Stability derivatives and modes of the aircraft are calculated by using the empirical formulas (Pamadi B. N. 2002) and confirmed by the XFLR5 software using Vortex Lattice Method. The root locus of the aircraft modes are shown in Figure 16. The detailed stability properties of the aircraft are tabulated in Table 6.

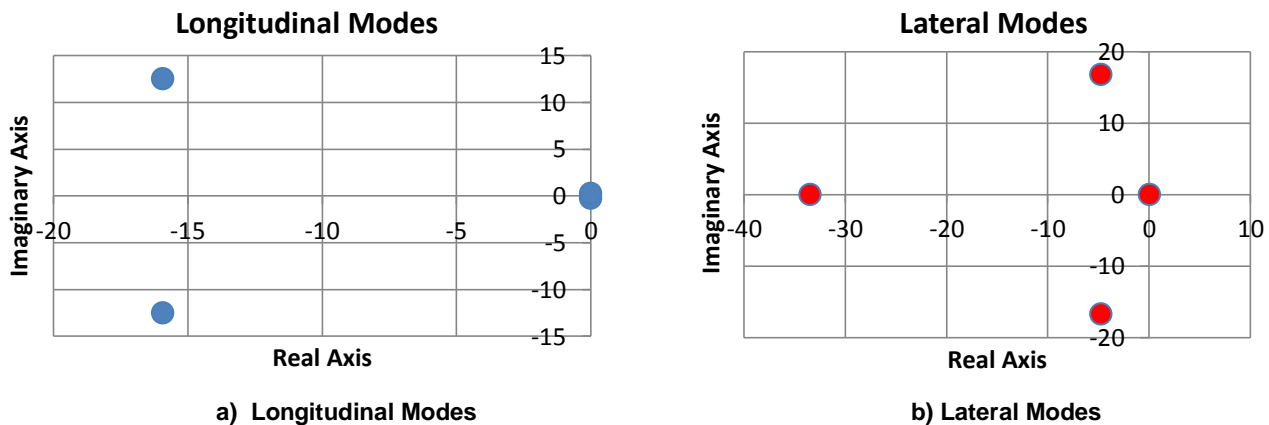


Figure 16: Stability modes of the aircraft

Table 6: Dynamic Stability analysis results

Stability Analysis			
Analysis Conditions		Longitudinal Modes	
Mass [kg]	1.96	λ_1	-15.92081- 12.50763i
I_{xx} [kg.cm ²]	1.34E+05	Damping Ratio	0.79
I_{yy} [kg.cm ²]	2.49E+05	Nat Freq. (rad/s)	20.24
I_{zz} [kg.cm ²]	3.78E+05	λ_2	-15.92081+ 12.50763i
I_{xz} [kg.cm ²]	2980	Damping Ratio	0.79
V_∞ [m/s]	19.69	Nat Freq. (rad/s)	20.24
Non-Dim. Stability Derivatives		λ_3	-0.00554- 0.25853i
C_{xu}	-0.00296	Damping Ratio	0.02
C_{Lu}	0.00001	Nat Freq. (rad/s)	0.26
C_{mu}	0	λ_4	-0.00554+ 0.25853i
C_{xa}	0.02595	Damping Ratio	0.02
C_{La}	4.17436	Nat Freq. (rad/s)	0.26
C_{ma}	-0.38054	Lateral Modes	
C_{xq}	0.03332	λ_1	-33.44938+ 0.00000i
C_{Lq}	5.73889	Time Constant (s)	0.03
C_{mq}	-4.7822		
C_{Yb}	-0.34205	λ_2	-4.76446- 16.74301i
C_{lb}	-0.00692	Damping Ratio	0.27
C_{nb}	0.19713	Nat Freq. (rad/s)	17.41
C_{Yp}	0.00063	λ_3	-4.76446+ 16.74301i
C_{lp}	-0.38808	Damping Ratio	0.27
C_{np}	-0.00822	Nat Freq. (rad/s)	17.41
C_{Yr}	0.44195	λ_4	0.02377+ 0.00000i
C_{lr}	0.04451	Time Constant (s)	42
C_{nr}	-0.25673		

All longitudinal poles are in stable region (Figure 16). Short period mode has high natural frequency and high damping ratio than phugoid mode. Both modes are oscillatory stable due to the imaginary parts of the poles. Short period mode response is faster than phugoid mode response.

Except one eigenvalue, all poles are in stable region. First eigenvalue represents roll mode and second and third one represent dutch roll mode, and finally last one represents spiral mode. Although the pole of spiral mode is in unstable region, pilot can recover easily since the time constant is 42 seconds.

Moreover, tail geometry is finalized by using this software. Proper vertical and horizontal tail areas are projected into the V tail arrangement. Zero flight path angle flight and a proper CG location is determined by theoretically and optimized with flight tests afterwards.

Detailed Drawings

After design is fixed and all the sizing calculations are done, all of the aircraft subsystems, connections, components, manufacturing tools, and payload mount systems are drawn in detail. Figure 17 shows the detailed drawings.

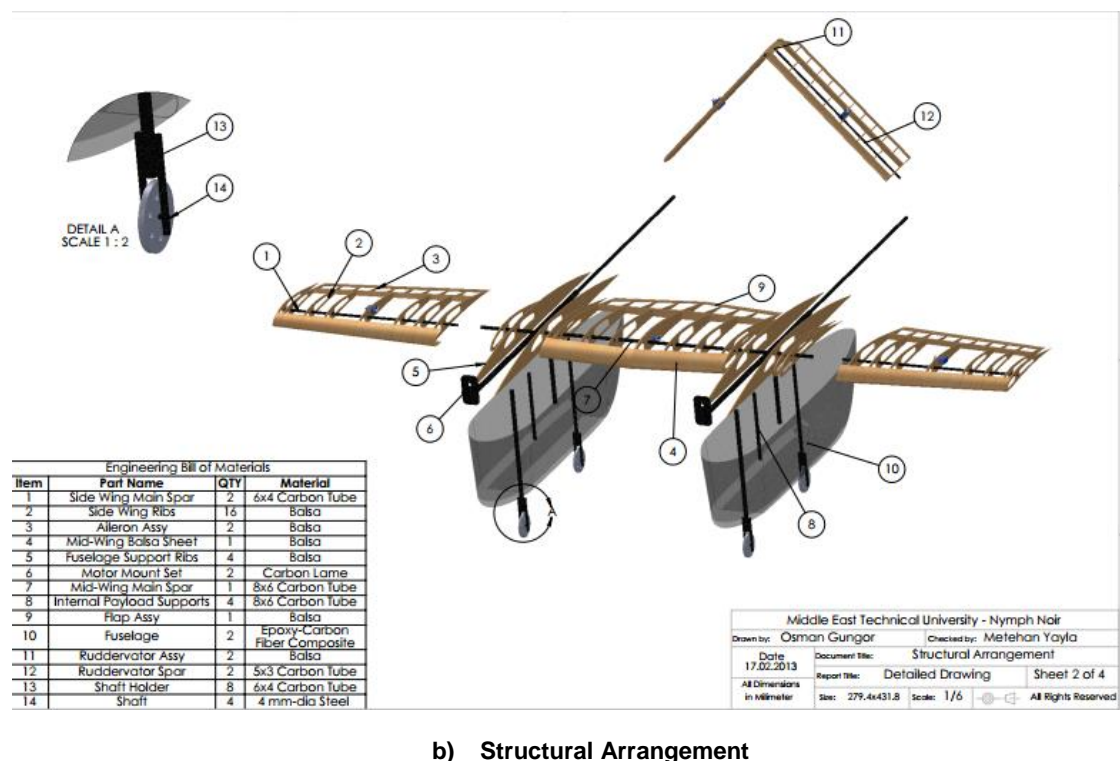
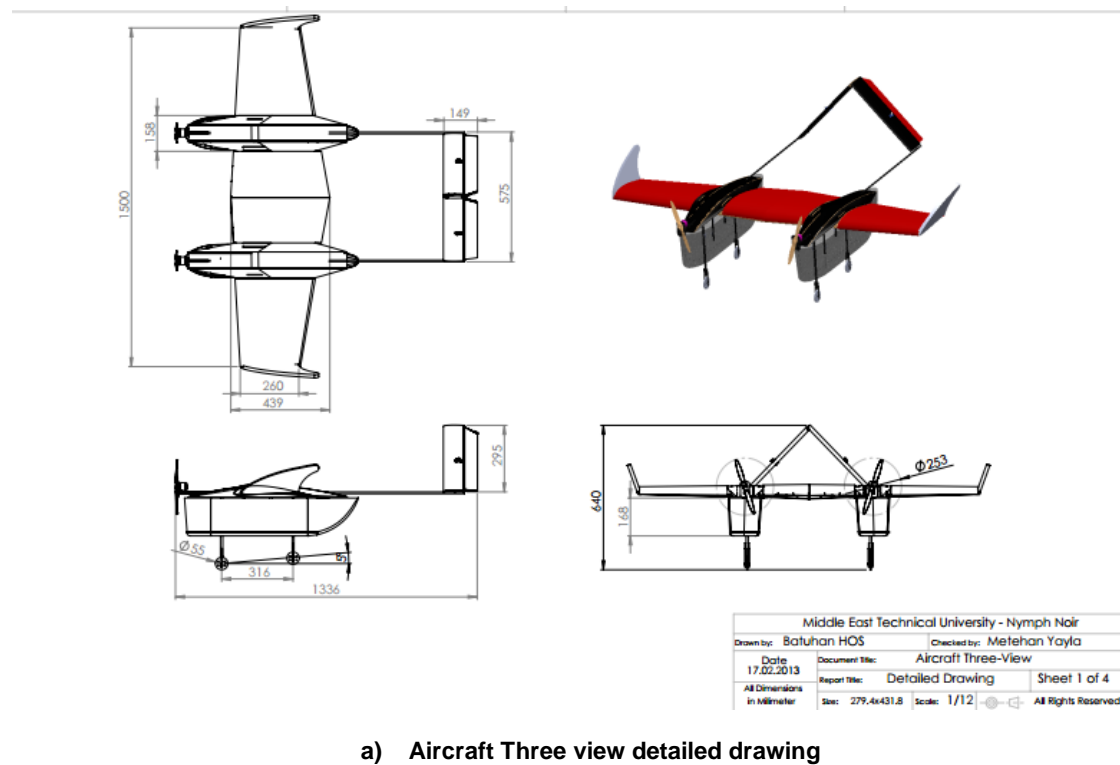


Figure 17: Detailed drawing of the aircraft

MANUFACTURING

In the manufacturing stage, to keep the aircraft as light as possible, choosing the best material and manufacturing method is of primary importance. By considering these important facts, totally 4 aircrafts with 3 prototypes are manufactured. These are manufactured by following a manufacturing time schedule.

By comparing, various selections of materials and manufacturing methods, the aircraft is manufactured as light as possible. The wings and tails are produced from balsa wood using the wing manufacturing tool and the leading edges of the tail and wings are produced with balsa wood sheeting. Fuselage is manufacturing with hybrid composite method which is include simple composite manufacturing techniques. Finally, the connections of carbon fiber frames, wings and fuselages are done with the help of epoxy and carbon fiber wrapping technique which is a procedure like tightly wrapping a connection point with wetted carbon fiber.



Figure 18: Sample Photos from Manufacturing Processes

FLIGHT TESTS & PERFORMANCE RESULTS

Performance of the aircraft is checked by using both Mathematical model in MATLAB based on Newton's 2nd Law and performance calculations based on the blade element methods. A summary of the aircraft flight performance is shown in Table 7.

In the first design, there were some failures observed during the flight tests such as: the aircraft was not able to take off in the given prescribed take-off area, the flow separated around the wing, etc... These were the main circumstances that made the aircraft configuration change from single engine configuration to twin engine configuration. The final design configuration of the aircraft is done based on these previous designs. Flight performance described in Table 7 is calculated based on the final design of the aircraft.

Table 7: Summary of Calculated Flight Performances

	Mission 1	Mission 2	Mission 3					
			Dice 1	Dice 2	Dice 3	Dice 4	Dice 5	Dice 6
$C_{L,max}$	1.757	1.757	1.757	1.757	1.757	1.757	1.757	1.757
$C_{L,cruise}$	0.012	0.02	0.02	0.02	0.02	0.02	0.02	0.02
e	0.934	0.934	0.934	0.934	0.934	0.934	0.934	0.934
$C_{D,0}$	0.02	0.02	0.021	0.021	0.021	0.02	0.021	0.021
$(L/D)_{max}$	13.39	13.43	13.27	13.21	13.21	13.31	13.21	13.21
$(L/D)_{cruise}$	5.6	8.48	8.23	8.23	8.23	8.34	8.23	8.23
Gross Weight [kg]	1.963	3.323	3.423	3.423	3.423	3.423	3.423	3.423
Wing Loading	38.36	64.9	66.9	66.9	66.9	66.9	66.9	66.9
Cruise Speed [m/s]	25.8	24.9	24.91	24.91	24.91	24.91	24.91	24.91
Stall Speed [m/s]	6.34	8.26	8.38	8.38	8.38	8.38	8.38	8.38
Max. Turn Rate [rad/s]	3.24	1.49	1.44	1.44	1.44	1.44	1.44	1.44
Max. Climb Rate [m/s]	12.6	6.7	6.5	6.5	6.5	6.5	6.5	6.5
Total Flight Time [s]	240	106	107.78	108.4	107.78	106.56	107.78	107.78

Flight testing campaign consists of taxi tests, stable C.G. point verification, finding the trim point controls and mission simulations. Taxi tests are performed in order to check the landing gear wheel track and wheel base distances are safe. Afterwards, first flight tests are done in order to check the calculated C.G. location is correct or not. For all possible configurations a proper C.G. point is determined with which the aircraft flies with zero degrees of flight path angle without any trim during cruise. Following the stability tests mission simulation tests are started. Each possible mission flight pattern is flown. Performance results are compared with the theoretical results.

Table 8: Comparison of mission performances and Predictions

Mission 1	Actual # of Laps	Predicted # of Laps
	6	6
Mission 2	Actual # of Internals	Predicted # of Internals
	12	12
Mission 3	Actual Flight Time (sec)	Predicted Flight Time (sec)
Dice 1	149	138
Dice 2	138	140
Dice 3	142	138
Dice 4	144	136
Dice 5	140	138
Dice 6	136	138

Moreover, during these tests several GPS data were collected; including latitude, longitude, maximum ground speed, and minimum ground speed and AGL altitude. Using horse shoe heading method (Rogers, 2002) in Figure 19 true airspeed (TAS) of the aircraft was determined. Horse-shoe maneuver was performed at altitude of AGL 120 meters. Results are tabulated in Table 9. A detailed description of the test is given in Mutlu et al. (2013). GPS waypoint track from a mission simulation test is also illustrated in Figure 20.

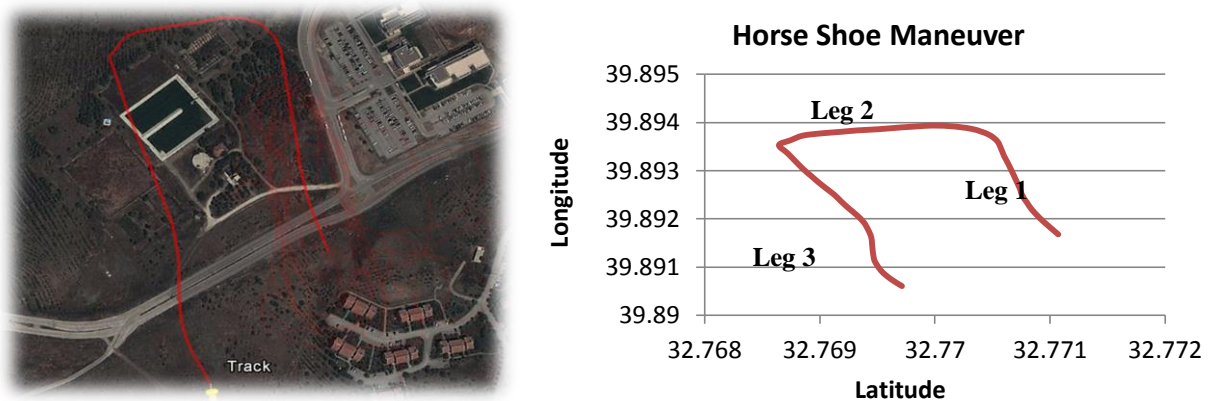


Figure 19: Horse Shoe Maneuver

Table 9: Horse Shoe Maneuver Test Results

	V_{G1} (m/s)	V_{G2} (m/s)	V_{G3} (m/s)	V_{Gmax} (m/s)	V_{wind} (m/s)	Wind Direction (Φ)	V_T (m/s)	V_{Tmax} (m/s)
Test Step	19.05	23.6	17.2	24.7	6.84	-62°	21.2	29.6



Figure 20: Mission Profile Drawn with GPS Data

Using correlations obtained from prescribed test step, three mission performances are obtained and tabulated in Table 10.

Table 9: Maximum TAS for Each Mission

	Mission 1	Mission 2	Mission 3					
			Dice 1	Dice 2	Dice 3	Dice 4	Dice 5	Dice 6
Max True Airspeed [m/s]	27.09	25.11	25.01	25.01	25.01	25.01	25.01	25.01
Estimated Max Speed [m/s]	25.8	24.9	24.91	24.91	24.91	24.91	24.91	24.91
Relative Error	%5	%0.86	%0.4	%0.86	%0.4	%0.4	%0.4	%0.4

Conducting a total number of 59 Flight tests (Figure 21) gives several feedbacks about design and the design is verified for the missions.



Figure 21: View from Flight tests

CONCLUSION

During an UAV design, one should consider the major requirement for design process. The constraints that are required for the aircraft should be considered in such a way that final design is able to satisfy the requirements. In the design process, it is better to divide major design process in 3 different stages as Conceptual Design, Preliminary Design, and Detailed Design. During each design process, it is better to check and see how the aircraft will be performed before starting the manufacturing. The design report is ranked 8th (Şenipek et al., 2013) and the designed aircraft is ranked as 10th among 81 competitors with mission 1 performance of 5 laps, mission 2 performance of 12 internal stores and unsuccessful flight attempt in mission 3. In the meantime, it is denoted that the team ranked first among the Turkish teams and all other international teams participated in the competition outside USA.



Figure 22: Nymph Noir Design Team and the Competition Aircraft, 2013

Acknowledgement

The sponsorship by ASELSAN, TAI, HAVELSAN, TEI, ROKETSAN, Ankara Governorship, METU and Turkish Airlines, are greatly acknowledged.

References

- Drela M., (2007) *QPROP analysis program for Propeller/Windmill Analysis and Design*, <http://web.mit.edu/drela/Public/web/qprop/>
- Mutlu T., Coşgun V., Yayla M., Sarsılmaz S. B., Tunca E., Kurtuluş B., Kurtuluş D. F., Tekinalp O. (2013) *Dynamic Stability Flight tests of Remote Sensing Measurement Capable Amphibious Unmanned aerial Vehicle (A-UAV)*, Ankara International Aerospace Conference, METU, Ankara
- Nicolai, L.M., Carichner, G.E. (2010) *Fundamentals of Aircraft and Airship Design*, AIAA, 2010
- Pamadi B. N. (2004) *Performance, Stability, Dynamics, and Control of Airplanes*, AIAA Educational Series
- Raymer, D.P. (1999). *Aircraft Design: A Conceptual Approach Fifth Edition*, AIAA Educational Series, 2012.
- Rogers, D.F.(2002) *Horseshoe Heading Technique*
- Senipek M. , Yayla M., Limon A. U., Rouzbar R. , Yosheph Y. , Kalkan U., Senol N., Akel E., Gungor O., Hos B., Usta A. Uzunlar I. O., Sarsilmaz S. B., Kurtulus D. F. (2013) *METU Nymph Noir Team AIAA DBF 2013 Design Report*, AIAA DBF Competition 2013, Tuscon, USA